Docosahexaenoic Acid Supplementation Represses the Early Immune Response Against Murine Cytomegalovirus but Enhances NK Cell Effector Function

Shuting Wu
Hunan Children's Hospital
Lili Wang
Hunan Children's Hospital
Hongyan Peng
Hunan Children's Hospital
Shuju Zhang
Hunan Children's Hospital
Qinglan Yang
Hunan Children's Hospital
Minghui Huang
Hunan Children's Hospital
Yana Li
Hunan Children's Hospital
Shuzhen Guan
Hunan Children's Hospital
Wenjuan Jiang
Hunan Children's Hospital
Zhaohui Zhang
Army Medical University, Third Military Medical University
Qinghua Bi
Army Medical University, Third Military Medical University
Liping Li
Hunan Children's Hospital
Yuan Gao
Army Medical University, Third Military Medical University
Peiwen Xiong
Hunan Children's Hospital
Zhaoyang Zhong
Army Medical University (Third Military Medical University)

Bo Xu
Xuzhou Medical University
Yafei Deng
Hunan Children's Hospital
Youcai Deng (youcai.deng@tmmu.edu.cn)
Army Medical University, Third Military Medical University

Research Article

Keywords: Docosahexaenoic acid, Cytomegalovirus, Natural killer cell, Mitochondrial activity, T cell activation.

Posted Date: November 17th, 2021

DOI: https://doi.org/10.21203/rs.3.rs-1057211/v1

Version of Record: A version of this preprint was published at BMC Immunology on April 19th, 2022. See the published version at https://doi.org/10.1186/s12865-022-00492-6.

Abstract

Background

Docosahexaenoic acid (DHA) supplementation is beneficial for several chronic diseases; however, its effect on immune regulation is still debated. Given the prevalence of cytomegalovirus (CMV) infection and because natural killer (NK) cells are the component of innate immunity critical for controlling CMV infection, the current study explored the effect of a DHA-enriched diet on susceptibility and the NK cell effector response to murine (M) CMV infection.

Results

Male C57BL/6 mice fed a control or DHA-enriched diet for 3 weeks were infected with MCMV and sacrificed at the indicated time points postinfection. Compared with control mice, DHA-fed mice had higher liver and spleen viral loads on day 7 postinfection, but final MCMV clearance was not affected. The ratio and total numbers of NK cells and their terminal mature cell subset ($KLRG1^+$ and $Ly49H^+$ NK cells) were reduced compared with those in control mice on day 7 but not day 21 postinfection. DHA feeding resulted in higher IFN-γ and granzyme B expression in splenic NK cells on day 7 postinfection. A mechanistic analysis showed that the splenic NK cells of DHA-fed mice showed enhanced glucose uptake, increased CD71 and CD98 expression, and higher mitochondrial mass and activity than those of control mice. In addition, DHA-fed mice showed reductions in the total numbers and activation of $CD4^+$ and $CD8^+$ T cells.

Conclusions

These results suggest that DHA supplementation represses the early response to CMV infection but preserves NK cell effector functions by improving mitochondrial activity, which may play critical roles in subsequent MCMV clearance.

Background

Dietary ω-3 polyunsaturated fatty acids (PUFAs) are abundant in nature and belong to a category of safety supplements that has been linked to a reduced risk of chronic diseases, such as cardiovascular diseases [1], cognitive decline [2] and cancer [3]. ω-3 PUFA supplementation during pregnancy also reduces the risks of premature birth and perinatal death and improves birth weight and neonatal growth and development [4]. Due to these health benefits, ω-3 PUFAs supplementation for the prevention of several diseases is on the rise [5, 6]. However, the public is still confused about the benefit of ω-3 PUFAs due to contradictory findings on the immunosuppressive effects of ω-3 PUFAs against viral or bacterial infection. For example, dietary supplementation with fish oil, which is enriched in ω-3 PUFAs, has been shown to impair host resistance to *Mycobacterium tuberculosis* [7] and influenza in mice [8]. However, the

lungs of mice whose diets were supplemented with only docosahexaenoic acid (DHA) and eicosapentaenoic acid (EPA), two main ω-3 PUFAs, had a lower *M. tuberculosis* bacterial load than those of controls [9, 10]. DHA-derived lipids, such as protectin D1 and protectin D1 isomers, have also been shown to suppress influenza virus replication and promote inflammation resolution [11]. This evidence suggests a multiple roles of ω-3 PUFAs in the immune response against bacterial or viral infection, warranting further in-depth study.

Cytomegalovirus (CMV), a member of the viral family known as herpesviruses, is a widespread virus, as approximately 45~100% of the global population has been exposed to CMV [12]. Noticeably, CMV infection is the most common and serious opportunistic infection in individuals with human immunodeficiency virus infection or patients after hematopoietic stem cell or solid organ transplantation [13]. As the critical component of innate immunity, natural killer (NK) cells play critical roles in controlling CMV viral replication, and experimental depletion of NK cells led to unchecked viral replication and increased mortality [14]. NK cells undergo a nonselective phase mediated by proinflammatory cytokines and a specific phase driven by signaling *via* Ly49H, an NK cell activation receptor that can directly recognize the MCMV-encoded protein m157 expressed on infected cells. The recognition of Ly49H by its ligand, m157, results in the robust expansion of $Ly49H^+$ NK cells, accompanied by the persistent elevation of KLRG1 [15]. NK cells also play critical roles in regulating steps of the adaptive immune response, such as T cell activation [16]. However, the effects of DHA supplementation on resistance against MCMV infection and the NK cell response remain largely unknown.

In the current study, we explored the susceptibility of C57BL/6 mice fed a DHA-enriched diet for 3 weeks to MCMV infection and assessed the homeostasis and maturation of NK cells in each tissue. We also explored the expression of molecules related to NK cell effector function and mitochondrial activity. Here, we show that DHA supplementation led to a reduced response to MCMV at the early but not later stage after infection. In addition, DHA supplementation preserved NK cell effector functions by improving metabolic status and mitochondrial activity, which may play critical roles in MCMV clearance in the later stage of infection.

Results

DHA supplementation inhibited the early but not later response to MCMV infection

To explore the effects of DHA on the susceptibility of mice to MCMV infection, 5-week-old C57BL/6 mice were first fed a special DHA-enriched or control diet for three weeks. After that, the mice were challenged with 3×10^4 PFU of MCMV in 200 μL of PBS by intraperitoneal injection and sacrificed on day 3, 7 or 21 (Fig. 1A). As the main markers of illness severity following MCMV infection, weight loss, the virus replication level, the visceral coefficient, and the local tissue mRNA levels of inflammatory cytokines were determined at the indicated time postinfection [17, 18]. We found that body weight loss was significantly

lower on day 3 but higher on days 5 and 7 after MCMV infection in DHA-fed mice than in control mice. However, there was no significant difference in body weight loss between control and DHA-fed mice on days 9, 14 and 21 after MCMV infection (Fig. 1B).

The spleen and liver are the two main target organs of MCMV after intraperitoneal infection [19], and our data showed that the levels of MCMV *IE-1* DNA were increased in both the spleen and liver tissues on day 7 but not day 3 postinfection. At the dose of MCMV given, no MCMV *IE-1* DNA was detected on day 21 postinfection in the spleen or liver in either the control or DHA-fed mice (Fig. 1C).

Viral infection is often accompanied by hepatosplenomegaly [20, 21]. Regarding the spleen/body weight and liver/body weight index, neither the spleen/body weight nor the liver/body weight was significantly different between control and DHA-fed mice on day 3 postinfection, but liver/body weight was significantly lower and spleen/body weight was decreased in DHA-fed mice compared with control mice on day 7 postinfection (Fig. 1D). Interestingly, in control mice, both spleen/body weight and liver/body weight index were significantly increased on day 7 postinfection compared with day 3 postinfection. When these two indexes on days 7 and day 3 postinfection in DHA-fed mice were compared, neither index was dramatically increased in DHA-fed mice compared with control mice (Fig. 1D). H&E staining showed that the pathology of both the spleen and liver was not obviously different between control and DHA-fed mice on day 7 postinfection (Fig. 1E).

All these findings demonstrated that DHA supplementation impaired the early response to MCMV infection without affecting final MCMV clearance at the later stage.

DHA feeding affected NK cell homeostasis, maturation and selective Ly49H expansion in the response to MCMV infection

As the NK cell number peaks on day 7 after MCMV infection [22], we next explored the homeostasis and maturation of NK cells on day 7 after MCMV infection. We analyzed the proportion and numbers of NK cells in the BM, spleen, pLNs, and liver tissue. Compared with those in control mice, both the proportion and total numbers of NK cells ($CD3^-CD19^-NK1.1^+NKp46^+$ among $CD45^+$ cells) were significantly decreased in the spleen but not other organs or tissues, although a similar trend without statistical significance was observed in the BM (Fig. 2A).

In response to MCMV infection, NK cells undergo accelerated phenotypic maturation [22]. When the maturation of NK cells was investigated based on the expression of CD27 and CD11b [23], terminal matured NK cells, indicated as $CD27^-CD11b^+$ NK cells, were significantly reduced in the BM, spleen and liver, whereas immature NK cells, indicated as $CD27^+CD11b^-$ NK cells, were significantly increased in the spleen and liver of DHA-fed mice compared with control mice (Fig. 2B). We also determined the expression levels of KLRG1, another marker of NK cell terminal maturation [24], and found that it was also elevated on NK cells after MCMV infection [22]. Our data showed that compared with control mice, DHA-fed mice exhibited significantly reduced $KLRG1^+$ NK cells in the BM, spleen and liver (Fig. 2C). Regarding the specific phase driven by Ly49H recognition [15], our data showed that DHA-fed mice had a

significantly reduced ratio and total number of Ly49H$^+$ NK cells in the spleen compared with those in control mice (Fig. 2D). However, there was no significant difference in the expression of CD11b, 27, KLRG1 or Ly49H on day 21 postinfection between control and DHA-fed mice (Fig. 2E).

All these data indicate that DHA supplementation affected NK cell homeostasis and repressed NK cell maturation and Ly49H$^+$ NK cell expansion in the main organs targeted in MCMV, such as the spleen and liver, at the early stage but not the later stage of MCMV infection.

DHA-fed mice showed an enhanced capacity for IFN-γ production and degranulation by NK cells during MCMV infection

Early during the course of infection, NK cells exert antiviral effects through direct toxicity and secretion of IFN-γ [25]. Therefore, we next tested the ratio of IFN-γ$^+$ NK cells after *in vitro* stimulation with PMA and ionomycin and determined the levels of the NK cell degranulation-related molecules perforin and granzyme B [26]. Our data revealed that the overall proportion and mean fluorescence intensity (MFI) of IFN-γ-secreting NK cells were increased in DHA-fed mice compared with control mice (Fig. 3A). The overall proportion and MFI of granzyme B, but not perforin, among splenic total NK cells were also increased in DHA-fed mice compared with control mice (Fig. 3B-C). These data suggest that DHA may improve NK cell effector function, although it represses NK cell expansion and maturation during MCMV infection.

DHA feeding improved the cellular metabolic status and mitochondrial activity of NK cells during MCMV infection

To explore the potential mechanism underlying the enhanced NK cell effector function induced by *in vivo* DHA supplementation, we next tested whether DHA feeding interfered with NK cell metabolic status, a basic process critical for facilitating robust NK cell effector functions [27]. NK cell activation results in an increase in the rates of both glycolysis and mitochondrial oxidative phosphorylation (OXPHOS). The expression levels of dedicated transporters, including the transferrin receptor CD71 and amino acid transporter CD98 [27], which control cellular access to nutrients, were substantially increased on the surface of NK cells from the DHA-fed mice compared with control mice on day 7 postinfection (Fig. 4A, B). Glucose uptake, indicated by the fluorescent glucose analog 2-(N-(7-nitrobenz-2-oxa-1,3-diazol-4-yl) amino)-2-deoxyglucose (2-NBDG) [28], was also increased in NK cells from the DHA-fed mice compared with control mice on day 7 postinfection (Fig. 4C).

Mitochondria, the essential hub of metabolic activity, are critical for OXPHOS activity and powerhouses of immunity [29]. In general, healthy mitochondria generate a proper membrane potential for the movement of substrates from the cytosol into the mitochondrial matrix for OXPHOS [30]. We found that on day 7 postinfection, splenic NK cells from DHA-fed mice had an increased overall mitochondrial content and increased mitochondrial membrane potential, as indicated by flow cytometric labeling with MitoTracker and TMRE, respectively (Fig. 4D, E).

Taken together, these findings suggest an increased overall rate of cellular metabolism and increased mitochondrial activity in NK cells from DHA-fed mice.

DHA feeding impaired the cellularity and activation of T cells in the spleen

As the above data showed that DHA feeding inhibited NK cell expansion, we decided to determine whether DHA feeding would affect cells of the adaptive immune response, such as T cells and B cells. The data showed that DHA feeding resulted in reduced proportions and numbers of total T cells and subsets of $CD4^+$ and $CD8^+$ T cells but had not obvious effect on B cell number (Fig. 5A).

To further determine whether DHA feeding affects T cell activation, we also measured the ratio of $CD62L^{hi}CD44^{lo}$ cells and $CD62L^{lo}CD44^{hi}$ cells, which represent naïve and activated T cells, respectively [31], among $CD4^+$ and $CD8^+$ T cells in both control and DHA-fed mice. We found an increased proportion of $CD44^-CD62L^+$ cells but a decreased proportion of $CD62L^+CD44^-$ cells among both $CD4^+$ T cells and $CD8^+$ T cells in DHA-fed mice compared with controls (Fig. 5B).

These data demonstrate that DHA feeding also impaired T cell expansion and activation.

DHA feeding influenced the mRNA expression of inflammatory mediators in the spleens of MCMV-infected mice

Coordinated secretion of cytokines and chemokines occurs in the target organ during MCMV infection [32]. To explore whether DHA feeding could influence the expression of various inflammatory mediators, the mRNA levels of these inflammatory mediators in splenic tissue were determined. The data showed significantly increased mRNA levels of *IL-4* but significantly decreased mRNA levels of *TNF-α* in the spleens of DHA-fed mice compared with controls. The mRNA levels of *MIP-1α* (also called CCL3) and *MCP-1* (also called CCL2) tended to be lower in the spleens of DHA-fed mice compared with controls, although the difference was not statistically significant (Fig. 6). Overall, these data suggest that DHA feeding led to a relatively immunosuppressive microenvironment on day 7 after MCMV infection.

Discussion

The use of dietary ω-3 PUFA supplementation for the prevention of chronic diseases is increasing due to the anti-inflammatory properties of ω-3 PUFAs. Generally, inflammation is also required for the clearance of invading pathogens, and indeed, some experimental studies have suggested that ω-3 PUFA supplementation impairs the clearance of some bacteria or viruses [7, 8]. However, a recent updated meta-analysis revealed that clinical omega-3 fatty acid supplementation is associated with favorable outcomes in patients with sepsis [9]. Additionally, a recent pilot study of 100 patients infected with SARS-CoV-2 suggests that higher levels of two major ω-3 PUFAs, DHA and EPA, are negatively correlated with the risk of COVID-19 mortality [33]. In the current study, we found that supplementation with DHA, the main component of ω-3 PUFAs, led to a reduced acute response against MCMV infection, as indicated by increases in weight loss and MCMV DNA load on day 7 postinfection, the early stage after MCMV

infection. Consistently, DHA feeding mitigated the inflammatory response at the same time after MCMV infection in MCMV-resistant C57BL/6 mice. However, DHA feeding did not affect the later stage of MCMV clearance in C57BL/6 mice. These findings suggest that DHA supplementation was more beneficial than harmful with respect to infection because although it delays the clearance of infection, it alleviates organ injury by mitigating the inflammatory response.

Consistent with the higher MCMV DNA load in DHA-fed mice, DHA supplementation also reduced the cell numbers and activation of NK cells and T cells, critical cellular components for MCMV clearance, and mitigated cytokine/chemokine levels on day 7 postinfection. The expression of KLRG1, an indicator of NK cell maturation activation and the response against MCMV infection, and the expression of Ly49H, an important protein in NK cells that acts against MCMV infection, was also reduced by DHA supplementation on day 7 postinfection. Consistently, during influenza virus infection, fish oil feeding led to a decrease in the numbers of NK cells and T lymphocytes in the lungs [34]. DHA feeding mitigated the levels of cytokines/chemokines, such as TNF-α, CCL3, and CCL-2, and reduced NK cell and T cell recruitment and activation after MCMV infection [35]. In addition, NK cells can secrete chemokines such as CCL3 and CCL4, which help shape and regulate adaptive immune responses [36]. Additionally, the reduction in NK cells induced by DHA feeding may contribute to decreased T cell number and activation. Therefore, understanding the complex crosstalk among NK cells, T cells and cytokines/chemokines regulated by DHA feeding needs further in-depth investigation.

NK cells also play critical roles in shaping processes of the adaptive immune response, such as T cell activation, during viral infection [16]. NK cells can directly or indirectly regulate the T cell response through the direct killing of infected cells and through cytokine secretion, respectively. Direct NK-dendritic cell (DC) interactions enhanced by NK cell-mediated IFN-γ and TNF production lead to upregulation of the costimulatory molecules CD86, CD83, CD80, human leukocyte antigen-DR (HLA-DR), and C-C chemokine receptor type 7 (CCR7) on DCs, which in turn results in enhanced $CD8^+$ T cell effector function. NK cell-derived IFN-γ can also directly induce $CD4^+$ T cell differentiation into T helper 1 cells, which facilitates the control of bacterial or virus infection [16]. Our data revealed that DHA-fed mice showed an enhanced capacity for IFN-γ production and increased expression of the cytotoxicity-related molecule granzyme B by NK cells on day 7 postinfection. This suggests that the preservation of NK cell effector function may play a critical role in the subsequent clearance of MCMV in the later stage of MCMV infection, partly by enhancing the adaptive immune response.

The increase in per-cell NK cell effector function by DHA feeding could be explained by metabolic reprogramming, a key issue involved in regulating NK cell activation and functional maintenance [27]. Our data showed that the uptake of NK cell nutrients, indicated by the enhanced uptake of the glucose analog 2-NBDG and improved expression of the nutrient receptors CD71 and CD98, was enhanced by DHA supplementation. The mitochondrial mass and membrane potential of NK cells in the mice fed DHA were also significantly improved after MCMV infection compared with those in the control mice. This might be the direct effect of DHA or its derivatives, such as resolvin D1 (RvD1) produced by 15-LOX and 5-LOX and MCTR1 catalyzed by 12-LOX, on mitochondria. The consumption of DHA or other ω-3 PUFAs could

remodel the mitochondrial phospholipidome and target mitochondrial enzymatic activity. For example, DHA acts as an agonist of PPARγ, which can promote mitochondrial biogenesis and induce the expression of genes encoding several key mitochondrial enzymes within mitochondria [37]. Dietary supplementation with fish oil for MCMV infection promoted mitochondrial biosynthesis in the liver cells of male C57BL/6 mice [38]. Both RvD1 and MCTR1 have been reported to improve mitochondrial biogenesis and function induced by multiple adverse factors, such as inflammation or high sugar [39–41].

Conclusions

In summary, although DHA supplementation resulted in an inhibited early response to MCMV infection, it preserved NK cell effector functions by improving mitochondrial activity, guaranteeing sufficient subsequent MCMV clearance in the later stage of infection. Therefore, DHA supplementation is more beneficial than harmful in the context of MCMV infection.

Materials And Methods

Animals

Five-week-old, male, wild-type (WT) C57BL/6J mice were purchased from Hunan Sja Laboratory Animal Co., Ltd. (Changsha, Hunan, China). All mice were housed under specific pathogen-free conditions at the Hunan Children's Hospital Animal Facility on a 12-hour light/dark schedule with free access to food and water. All animal procedures and protocols were approved by the Animal Ethics Committee of Hunan Children's Hospital and followed the guidelines of the Institutional Animal Care and Use Committees of Hunan Children's Hospital (Changsha, Hunan, China).

Virus Stock Preparation

The MCMV strain Smith (VR-1399) was a kind gift from the College of Life Sciences, Hunan Normal University (Changsha, Hunan, China). Stocks of MCMV Smith strain salivary gland extracts were prepared as previously described [42]. Viral titer is expressed in plaque-forming units (PFU)/mL. BALB/c mice were infected with 5×10^3 PFU of virus through intraperitoneal injection and euthanized 2 weeks later. All mice were sacrificed by cervical dislocation under anesthesia by 2% pentobarbital sodium. The salivary glands were collected and homogenized to obtain initial salivary gland-derived MCMV, and these steps were then repeated at least 3 times to obtain more virulent virus. PFUs were quantitated by a simple plaque-forming cell assay on 3T3 fibroblasts provided by Dr. Chen Ze (College of Life Sciences, Hunan Normal University, Changsha, Hunan, China) as previously described [43].

Dha Diet And Cmv Infection

Five-week-old, male C57BL/6J mice consumed a control diet (D200208, Research Diets) or a diet containing DHA at physiological levels (2.48% DHA, D201124, Research Diets) ad libitum for 3 weeks (the ingredients of the diets are listed in Table 1.). Following 3 weeks of dietary treatment, the mice were infected with MCMV by intraperitoneal injection (3×10^4 PFU, diluted in 200 µL of PBS). The mice were weighed following infection, and the percent weight loss on days 0, 3, 7, 9, 14 and 21 after MCMV infection was calculated by comparison with the starting weight. Mice were by cervical dislocation under anesthesia by 2% pentobarbital sodium on day 3, 7 or 21 after MCMV infection for subsequent studies.

Table 1
Composition of experimental diets

Ingredient	**Control**		**DHA**	
	g/100g	kcal/100g	g/100g	kcal/100g
Caisein	20.000	80.000	20.000	80.000
DL-Methionine	0.300	1.200	0.300	1.200
Dyetrose	12.000	48.000	12.000	48.000
Cornstarch	51.800	207.200	51.800	207.200
Soybean Oil	6.200	55.800	3.720	33.480
DHA	0.000	0.000	2.480	22.320
Cellulose	5.000	0.000	5.000	0.000
Mineral Mix #200000	3.500	0.000	3.500	0.000
Vitamin Mix #300050	1.000	4.000	1.000	4.000
Choline Bitartrate	0.200	0.000	0.200	0.000
Red Dye	0.005	0.000	0.005	0.000

Quantification of MCMV IE-1 **DNA levels in the liver and spleen by Real-time Quantitative PCR (qPCR)**

Ten milligrams of fresh liver and spleen tissues were cut into small pieces and placed in a 1.5-ml microcentrifuge tube. DNeasy Blood & Tissue Kits (QIAGEN, 69504) were used for rapid purification of the total DNA. Real-time qPCR was performed using Bestar® SYBR Green qPCR Master Mix (DBI Bioscience, San Diego, CA, United States) with a Roche LightCycler® 480 II. The cycle threshold (Ct) values were used to calculate the DNA level by using the following expression: 2^{-Ct}/tissue weight (10 mg). The primer sequences specific for the immediate early gene (*IE-1*) used for qPCR were designed by Primer Bank and are as follows: MCMV *IE-1* Forward, 5'-TCGCCCATCGTTTCGAGA-3'; Reverse, 5'-TCTCGTAGGTCCACTGACGGA-3' [44].

Pathological Evaluation Of Spleen And Liver Tissues

The liver and spleen were removed on day 7 postinfection and fixed with 10% phosphate-buffered formalin, paraffin embedded, cut into 4-μm sections, and stained with hematoxylin and eosin, as described previously [45].

Preparation Of Single-cell Suspensions And Counts

Single-cell suspensions were prepared from the bone marrow (BM), spleen, peripheral lymph nodes (pLNs) and liver as described previously. The BM, spleens, pLNs and livers were ground and passed through a 40-μm nylon filter. The obtained liver cells were resuspended in 40% Percoll in RPMI 1640 medium containing 5% FBS and then centrifuged (2000 rpm, 4°C, 5 min). Cell pellets were resuspended in RPMI 1640 medium containing 5% FBS. The cells from each tissue were counted with an automated cell counter (Countstar IC1000).

Flow Cytometry

All antibodies purchased for flow cytometry are listed in Table 2. Standard protocols were followed for flow cytometry, as described previously [46]. All flow cytometry experiments were carried out on a BD LSRFortessa^{TM} cell analyzer, and data were analyzed with FlowJo software.

Table 2
Antibodies for Flow cytometry

Antibody	Clone	Source	Identifier
Anti-mouse-NK1.1	PK136	BioLegend	Cat#108708 Cat#108753
Anti-mouse NKp46	29A1.4	BioLegend	Cat#137618 Cat#137608
Anti-mouse CD11b	M1/70	BioLegend	Cat#101228
Anti-mouse KLRG1	2F11KLRG1	BioLegend	Cat#138414
Anti-mouse CD62L	MEL-14	BioLegend	Cat#104438
Anti-mouse CD45	30-F11	BioLegend	Cat#103154
Anti-mouse CD3	17A2	BioLegend	Cat#100216 Cat#100320
Anti-mouse CD19	605	BioLegend	Cat#115520 Cat#115528
Anti-mouse GZMB	GB11	BioLegend	Cat#515406
Anti-mouse perforin	S16009A	BioLegend	Cat#154306
Anti-mouse CD27	LG 3A10	eBioscience	Cat#124229
Anti- mouse CD16/32	2.4G2	BD Biosciences	Cat #553141
Anti-mouse Ly49H	3D10	BD	Cat#744262
Anti-mouse CD4	RM4-5	BD	Cat#550954
Anti-mouse CD8a	53-6.7	BD/Biolegend	Cat#553030 Cat#563898
Anti-mouse CD71	C2	BD	Cat#553266
Anti-mouse IFN-γ	XMG1.2	BD	Cat#554411
Anti-mouse CD98	RL388	Invitrogen	Lot#2074373
Anti-mouse CD44	IM7	BioLegend	Cat#103044

Briefly, to detect surface markers, cells were stained with antibodies in staining buffer (phosphate-buffered saline (PBS) containing 2% mouse serum, 2% horse serum, and anti-CD16/CD32 blocking antibodies) in the dark for 15 min at room temperature. For intracellular IFN-γ staining, cells were stimulated with phorbol 12-myristate 13-acetate (PMA) and ionomycin (eBioscience) plus BD Golgi Plug™ protein transport inhibitor (BD Biosciences) for 4 h, and the cells were then stained with reagent from a Fixation/Permeabilization Solution Kit (BD Biosciences) following the manufacturer's instructions.

To stain other intracellular proteins (including granzyme B and perforin), cells were stained with surface antibodies, permeabilized with reagent from a Foxp3/Transcription Factor Staining Buffer Set Kit

(eBioscience), and then stained with anti-granzyme B and anti-perforin antibody or isotype-matched control antibody.

To determine the glucose uptake capacity of NK cells, the cells were cultured with prewarmed (37°C) RPMI 1640 medium (Life Technologies) containing 100 μM 2-(N-(7-nitro-benz-2-oxa-1,3-diazol-4-yl) amino)-2-deoxyglucose (2-NBDG, a fluorescent glucose analog) (Invitrogen) for 10 min at 37°C in the dark.

To determine mitochondrial activity, splenic cells were cultured (37°C, 30 min) with prewarmed (37°C) RPMI 1640 medium containing 20 nM MitoTracker® Green FM (Invitrogen) or tetramethylrhodamine ethyl ester (TMRE) (Invitrogen) in the dark.

Quantitation Of Spleen Mrna Cytokine And Chemokine Levels

The spleens were removed from DHA-fed and control mice on day 7 postinfection. The TRIzol method was used to isolate the total RNA, and reverse transcription (RT) was conducted with Evo M-MLV RT Premix for qPCR (Accurate Biology). The mRNA levels of *TNF-α*, *IL-4*, *IL-6*, *IL-12*, *IL-10*, *IFN-α*, *IFN-β*, macrophage inflammatory protein-1-a (*MIP-1α*, also called *CCL3*), and monocyte chemotactic protein-1 (*MCP-1*, also called *CCL-2*) were measured using real-time qRT-PCR. The Ct values were normalized to the internal control. DNA levels was calculated by the following expression: ($2^{-\triangle Ct}$). The primer pairs used for qRT-PCR are listed in Table 3. Values reflecting the expression of each cytokine or chemokine obtained from different mice were averaged and scaled for normalization. Then, heatmaps were generated by using the 'ComplexHeatmap' package in R [47]. The complete linkage method was used to find similar clusters among cytokines and mice.

Table 3
Primers of cytokine and chemokine

Primer	Sequence (5’-3’)	References
TNF-α-F	TGCCTATGTCTCAGCCTCTTC	[48]
TNF-α-R	GGTCTGGGCCATAGAACTGA	[48]
IL-4-F	GGCATTTTGAACGAGGTCACA	[49]
IL-4-R	AGGACGTTTGGCACATCCA	[49]
IL-6-F	TGTGCAATGGCAATTCTGAT	[48]
IL-6-R	GGTACTCCAGAAGACCAGAGGA	[48]
IL-10-F	GCTCTTACTGACTGGCATGAG	[50]
IL-10-R	CGCAGCTCTAGGAGCATGTG	[50]
IL-12-F	GAGGTGGACTGGACTCCC	[51]
IL-12-R	GCAGGGAACACATGCCCA	[51]
IFN-α-F	TGTCTGATGCAGCAGGTGG	[52]
IFN-α-R	AAGACAGGGCTCTCCAGAC	[52]
IFN-β-F	CTGGCTTCCATCATGAACAA	[52]
IFN-β-R	CATTTCCGAATGTTCGTCCT	[52]
MCP-1-F	TTAAAAACCTGGATCGGAACCAA	[53]
MCP-1-R	GCATTAGCTTCAGATTTACGGG	[53]
MIP-1α-F	ATGAAGGTCTCCACCACTGCCCTTG	[54]
MIP-1α-R	GGCATTCAGTTCCAGGTCAGTGAT	[54]
IE-1-F	TCGCCCATCGTTTCGAGA	[44]
IE-1-R	TCTCGTAGGTCCACTGACGGA	[44]
GAPDH-F	AGGTCGGTGTGAACGGATTTG	[55]
GAPDH-R	TGTAGACCATGTAGTTGAGGTCA	[55]

Statistical analysis

The sample size was3 to 9 per group, and two or three independent experiments were performed for each experiment. Statistical analysis was carried out using SPSS 23.0 (Chicago, IL, United States). The data in this study are expressed as the mean ± standard deviation (SD). If the data were normally distributed, an unpaired two-tailed Student’s t test was used to analyze the differences between two independent groups.

Otherwise, a two-tailed Mann-Whitney U test was used to analyze the differences, and differences with a p value ≤ 0.05 are considered significant. All graphs were generated by GraphPad Prism 8.0 (GraphPad Software Inc., La Jolla, CA, United States).

Abbreviations

DHA: Docosahexaenoic acid; NK cells: natural killer; CMV: cytomegalovirus; MCMV: murine cytomegalovirus; PUFAs: polyunsaturated fatty acids; EPA: eicosapentaenoic acid; WT: wild-type; PFU: plaque-forming units; qPCR:Real-time Quantitative PCR; RT: reverse transcription; BM: bone marrow; pLNs: peripheral lymph nodes; PBS: phosphate-buffered saline; 2-NBDG: 2-(N-(7-nitro-benz-2-oxa-1,3-diazol-4-yl) amino)-2-deoxyglucose; TMRE: tetramethylrhodamine ethyl ester; OXPHOS: oxidative phosphorylation; RvD1: resolvin D1; MFI: Mean fluorescence index.

Declarations

Acknowledgements

Not applicable.

Funding

This study was supported by the National Natural Science Foundation of China (Nos. 81922068 and 81874313 to YoD; No. 81900055 to HP). This work was also supported by funding from the Natural Science Foundation of Changsha (No. kq2014185 to SW). This study was supported by grants from the Chongqing Science and Technology Commission of China (cstc2019jcyj-msxmX0502). This study was supported by funding from the National Key Research and Development Project (Nos. 2020YFA0113500 and 2019YFA0111200 to YoD). This study was also supported by funding from the Natural Science Foundation of Hunan Province (No. 2021JJ40274 to HP; No. 2020JJ5279 to YaD). This work was also supported by funding from the Science Foundation of Hunan Children's Hospital (2020 and 2021).

Availability of data and materials

All data are included in the manuscript.The datasets analyzed in the current study are available from thecorresponding author on reasonable request.

Ethics approvaland consent to participate

All methods in this current study are reported in accordance with ARRIVE guidelines. The studies involving animal procedures and protocols were approved by the Animal Ethics Committee of Hunan Children’s Hospital, and the ethics committee approval code wasHCHLL-2021-70. Thisstudy does not involve the use of human data or tissue.All experimentswere performed in accordance with relevant guidelines and regulations at Hunan Children’s Hospital. All mice weresacrificed by cervical dislocation under anesthesia by2% pentobarbital sodium.

Competing interests

The authors declare that they have no competing interests.

Consent for publication

Not applicable.

Authors' contributions

The work presented was performed in collaboration with all authors. SW designed and performed the experiments, analyzed the data, and wrote the manuscript. LW performed the experiments and analyzed the data. HP, SZ, QY, MH, YL, SG, WJ, ZZ, and QB performed the experiments. LL, YG, PX and ZZ designed the experiments and edited the manuscript. BX and YaD designed the research, performed the experiments and edited the manuscript. YoD devised the concept, designed the research, supervised the study, and wrote the manuscript.

References

1. Rimm EB, Appel LJ, Chiuve SE, Djousse L, Engler MB, Kris-Etherton PM et al. Seafood Long-Chain n-3 Polyunsaturated Fatty Acids and Cardiovascular Disease: A Science Advisory From the American Heart Association. Circulation. 2018; doi:10.1161/CIR.0000000000000574
2. Cardoso C, Afonso C, Bandarra NM. Dietary DHA and health: cognitive function ageing. Nutr Res Rev. 2016; doi:10.1017/S0954422416000184
3. Dierge E, Debock E, Guilbaud C, Corbet C, Mignolet E, Mignard L et al. Peroxidation of n-3 and n-6 polyunsaturated fatty acids in the acidic tumor environment leads to ferroptosis-mediated anticancer effects. Cell Metab. 2021; doi:10.1016/j.cmet.2021.05.016
4. Makrides M, Gibson RA, McPhee AJ, Yelland L, Quinlivan J, Ryan P et al. Effect of DHA supplementation during pregnancy on maternal depression and neurodevelopment of young children: a randomized controlled trial. JAMA. 2010; doi:10.1001/jama.2010.1507
5. Guu TW, Mischoulon D, Sarris J, Hibbeln J, McNamara RK, Hamazaki K et al. International Society for Nutritional Psychiatry Research Practice Guidelines for Omega-3 Fatty Acids in the Treatment of Major Depressive Disorder. Psychother Psychosom. 2019; doi:10.1159/000502652
6. Guo XF, Li KL, Li JM, Li D. Effects of EPA and DHA on blood pressure and inflammatory factors: a meta-analysis of randomized controlled trials. Crit Rev Food Sci Nutr. 2019; doi:10.1080/10408398.2018.1492901
7. Paul KP, Leichsenring M, Pfisterer M, Mayatepek E, Wagner D, Domann M et al. Influence of n-6 and n-3 polyunsaturated fatty acids on the resistance to experimental tuberculosis. Metabolism. 1997; doi:10.1016/s0026-0495(97)90003-2
8. Schwerbrock NM, Karlsson EA, Shi Q, Sheridan PA, Beck MA. Fish oil-fed mice have impaired resistance to influenza infection. J Nutr. 2009; doi:10.3945/jn.109.108027

9. Nienaber A, Baumgartner J, Dolman RC, Ozturk M, Zandberg L, Hayford FEA et al. Omega-3 Fatty Acid and Iron Supplementation Alone, but Not in Combination, Lower Inflammation and Anemia of Infection in Mycobacterium tuberculosis-Infected Mice. Nutrients. 2020; doi:10.3390/nu12092897
10. Jordao L, Lengeling A, Bordat Y, Boudou F, Gicquel B, Neyrolles O et al. Effects of omega-3 and -6 fatty acids on Mycobacterium tuberculosis in macrophages and in mice. Microbes Infect. 2008; doi:10.1016/j.micinf.2008.08.004
11. Imai Y. Role of omega-3 PUFA-derived mediators, the protectins, in influenza virus infection. Biochim Biophys Acta. 2015; doi:10.1016/j.bbalip.2015.01.006
12. Cannon MJ, Schmid DS, Hyde TB. Review of cytomegalovirus seroprevalence and demographic characteristics associated with infection. Rev Med Virol. 2010; doi:10.1002/rmv.655
13. Griffiths P, Reeves M. Pathogenesis of human cytomegalovirus in the immunocompromised host. Nat Rev Microbiol. 2021; doi:10.1038/s41579-021-00582-z
14. Bukowski JF, Woda BA, Welsh RM. Pathogenesis of murine cytomegalovirus infection in natural killer cell-depleted mice. J Virol. 1984; doi:10.1128/JVI.52.1.119-128.1984
15. Fogel LA, Sun MM, Geurs TL, Carayannopoulos LN, French AR. Markers of nonselective and specific NK cell activation. J Immunol. 2013; doi:10.4049/jimmunol.1202533
16. Crouse J, Xu HC, Lang PA, Oxenius A. NK cells regulating T cell responses: mechanisms and outcome. Trends Immunol. 2015; doi:10.1016/j.it.2014.11.001
17. Hraiech S, Bordes J, Mege JL, de Lamballerie X, Charrel R, Bechah Y et al. Cytomegalovirus reactivation enhances the virulence of Staphylococcus aureus pneumonia in a mouse model. Clinical microbiology and infection : the official publication of the European Society of Clinical Microbiology and Infectious Diseases. 2017; doi:10.1016/j.cmi.2016.09.025
18. Oakley OR, Garvy BA, Humphreys S, Qureshi MH, Pomeroy C. Increased weight loss with reduced viral replication in interleukin-10 knock-out mice infected with murine cytomegalovirus. Clinical and experimental immunology. 2008; doi:10.1111/j.1365-2249.2007.03533.x
19. Hsu KM, Pratt JR, Akers WJ, Achilefu SI, Yokoyama WM. Murine cytomegalovirus displays selective infection of cells within hours after systemic administration. J Gen Virol. 2009; doi:10.1099/vir.0.006668-0
20. Ferraz AC, Almeida LT, da Silva Caetano CC, da Silva Menegatto MB, Souza Lima RL, de Senna JPN et al. Hepatoprotective, antioxidant, anti-inflammatory, and antiviral activities of silymarin against mayaro virus infection. Antiviral Res. 2021; doi:10.1016/j.antiviral.2021.105168
21. Ishii T, Sasaki Y, Maeda T, Komatsu F, Suzuki T, Urita Y. Clinical differentiation of infectious mononucleosis that is caused by Epstein-Barr virus or cytomegalovirus: A single-center case-control study in Japan. J Infect Chemother. 2019; doi:10.1016/j.jiac.2019.01.012
22. Robbins SH, Tessmer MS, Mikayama T, Brossay L. Expansion and contraction of the NK cell compartment in response to murine cytomegalovirus infection. J Immunol. 2004; doi:10.4049/jimmunol.173.1.259

23. Chiossone L, Chaix J, Fuseri N, Roth C, Vivier E, Walzer T. Maturation of mouse NK cells is a 4-stage developmental program. Blood. 2009; doi:10.1182/blood-2008-10-187179
24. Narni-Mancinelli E, Vivier E. NK cell genesis: a trick of the trail. Immunity. 2012; doi:10.1016/j.immuni.2012.01.001
25. Quatrini L, Wieduwild E, Escaliere B, Filtjens J, Chasson L, Laprie C et al. Endogenous glucocorticoids control host resistance to viral infection through the tissue-specific regulation of PD-1 expression on NK cells. Nature immunology. 2018; doi:10.1038/s41590-018-0185-0
26. Fehniger TA, Cai SF, Cao X, Bredemeyer AJ, Presti RM, French AR et al. Acquisition of murine NK cell cytotoxicity requires the translation of a pre-existing pool of granzyme B and perforin mRNAs. Immunity. 2007; doi:10.1016/j.immuni.2007.04.010
27. O'Brien KL, Finlay DK. Immunometabolism and natural killer cell responses. Nat Rev Immunol. 2019; doi:10.1038/s41577-019-0139-2
28. Zou C, Wang Y, Shen Z. 2-NBDG as a fluorescent indicator for direct glucose uptake measurement. J Biochem Biophys Methods. 2005; doi:10.1016/j.jbbm.2005.08.001
29. Mills EL, Kelly B, O'Neill LAJ. Mitochondria are the powerhouses of immunity. Nat Immunol. 2017; doi:10.1038/ni.3704
30. Vyas S, Zaganjor E, Haigis MC. Mitochondria and Cancer. Cell. 2016; doi:10.1016/j.cell.2016.07.002
31. Gerberick GF, Cruse LW, Miller CM, Sikorski EE, Ridder GM. Selective modulation of T cell memory markers CD62L and CD44 on murine draining lymph node cells following allergen and irritant treatment. Toxicol Appl Pharmacol. 1997; doi:10.1006/taap.1997.8218
32. Biron CA, Tarrio ML. Immunoregulatory cytokine networks: 60 years of learning from murine cytomegalovirus. Med Microbiol Immunol. 2015; doi:10.1007/s00430-015-0412-3
33. Asher A, Tintle NL, Myers M, Lockshon L, Bacareza H, Harris WS. Blood omega-3 fatty acids and death from COVID-19: A pilot study. Prostaglandins Leukot Essent Fatty Acids. 2021; doi:10.1016/j.plefa.2021.102250
34. Gutierrez S, Svahn SL, Johansson ME. Effects of Omega-3 Fatty Acids on Immune Cells. Int J Mol Sci. 2019; doi:10.3390/ijms20205028
35. Salazar-Mather TP, Hokeness KL. Cytokine and chemokine networks: pathways to antiviral defense. Curr Top Microbiol Immunol. 2006; doi:10.1007/978-3-540-33397-5_2
36. Zitti B, Bryceson YT. Natural killer cells in inflammation and autoimmunity. Cytokine Growth Factor Rev. 2018; doi:10.1016/j.cytogfr.2018.08.001
37. Sullivan EM, Pennington ER, Green WD, Beck MA, Brown DA, Shaikh SR. Mechanisms by Which Dietary Fatty Acids Regulate Mitochondrial Structure-Function in Health and Disease. Adv Nutr. 2018; doi:10.1093/advances/nmy007
38. Rossignoli CP, Dechandt CRP, Souza AO, Sampaio IH, Vicentini TM, Teodoro BG et al. Effects of intermittent dietary supplementation with conjugated linoleic acid and fish oil (EPA/DHA) on body

metabolism and mitochondrial energetics in mice. J Nutr Biochem. 2018; doi:10.1016/j.jnutbio.2018.07.001

39. Zirpoli H, Sosunov SA, Niatsetskaya ZV, Mayurasakorn K, Manual Kollareth DJ, Serhan CN et al. NPD1 rapidly targets mitochondria-mediated apoptosis after acute injection protecting brain against ischemic injury. Exp Neurol. 2021; doi:10.1016/j.expneurol.2020.113495
40. Yang Y, Zhu Y, Xiao J, Tian Y, Ma M, Li X et al. Maresin conjugates in tissue regeneration 1 prevents lipopolysaccharide-induced cardiac dysfunction through improvement of mitochondrial biogenesis and function. Biochem Pharmacol. 2020; doi:10.1016/j.bcp.2020.114005
41. Trotta MC, Pieretti G, Petrillo F, Alessio N, Hermenean A, Maisto R et al. Resolvin D1 reduces mitochondrial damage to photoreceptors of primary retinal cells exposed to high glucose. J Cell Physiol. 2020; doi:10.1002/jcp.29303
42. Beaulieu AM, Sun JC. Tracking Effector and Memory NK Cells During MCMV Infection. Methods Mol Biol. 2016; doi:10.1007/978-1-4939-3684-7_1
43. Brune W, Hengel H, Koszinowski UH. A mouse model for cytomegalovirus infection. Curr Protoc Immunol. 2001; doi:10.1002/0471142735.im1907s43
44. Adams NM, Lau CM, Fan X, Rapp M, Geary CD, Weizman OE et al. Transcription Factor IRF8 Orchestrates the Adaptive Natural Killer Cell Response. Immunity. 2018; doi:10.1016/j.immuni.2018.04.018
45. Zhang Q, Deng Y, Lai W, Guan X, Sun X, Han Q et al. Maternal inflammation activated ROS-p38 MAPK predisposes offspring to heart damages caused by isoproterenol via augmenting ROS generation. Sci Rep. 2016; doi:10.1038/srep30146
46. Wang F, Meng M, Mo B, Yang Y, Ji Y, Huang P et al. Crosstalks between mTORC1 and mTORC2 variagate cytokine signaling to control NK maturation and effector function. Nat Commun. 2018; doi:10.1038/s41467-018-07277-9
47. Gu Z, Eils R, Schlesner M. Complex heatmaps reveal patterns and correlations in multidimensional genomic data. Bioinformatics. 2016; doi:10.1093/bioinformatics/btw313
48. Hashimoto-Kataoka T, Hosen N, Sonobe T, Arita Y, Yasui T, Masaki T et al. Interleukin-6/interleukin-21 signaling axis is critical in the pathogenesis of pulmonary arterial hypertension. Proc Natl Acad Sci U S A. 2015; doi:10.1073/pnas.1424774112
49. Banda NK, Thurman JM, Kraus D, Wood A, Carroll MC, Arend WP et al. Alternative complement pathway activation is essential for inflammation and joint destruction in the passive transfer model of collagen-induced arthritis. J Immunol. 2006; doi:10.4049/jimmunol.177.3.1904
50. Rajasekaran M, Sul OJ, Choi EK, Kim JE, Suh JH, Choi HS. MCP-1 deficiency enhances browning of adipose tissue via increased M2 polarization. J Endocrinol. 2019; doi:10.1530/JOE-19-0190
51. Bohn E, Autenrieth IB. IL-12 is essential for resistance against Yersinia enterocolitica by triggering IFN-gamma production in NK cells and CD4+ T cells. J Immunol. 1996;
52. Lienenklaus S, Walisko R, te Boekhorst A, May T, Samuelsson C, Michiels T et al. PCR-based simultaneous analysis of the interferon-alpha family reveals distinct kinetics for early interferons. J

Interferon Cytokine Res. 2008; doi:10.1089/jir.2008.0082

53. Miyabe C, Miyabe Y, Bricio-Moreno L, Lian J, Rahimi RA, Miura NN et al. Dectin-2-induced CCL2 production in tissue-resident macrophages ignites cardiac arteritis. J Clin Invest. 2019; doi:10.1172/JCI123778
54. Reiner SL, Zheng S, Wang ZE, Stowring L, Locksley RM. Leishmania promastigotes evade interleukin 12 (IL-12) induction by macrophages and stimulate a broad range of cytokines from CD4+ T cells during initiation of infection. J Exp Med. 1994; doi:10.1084/jem.179.2.447
55. Deng Y, Yang Q, Yang Y, Li Y, Peng H, Wu S et al. Conditional knockout of Tsc1 in RORgammat-expressing cells induces brain damage and early death in mice. J Neuroinflammation. 2021; doi:10.1186/s12974-021-02153-8

Figures

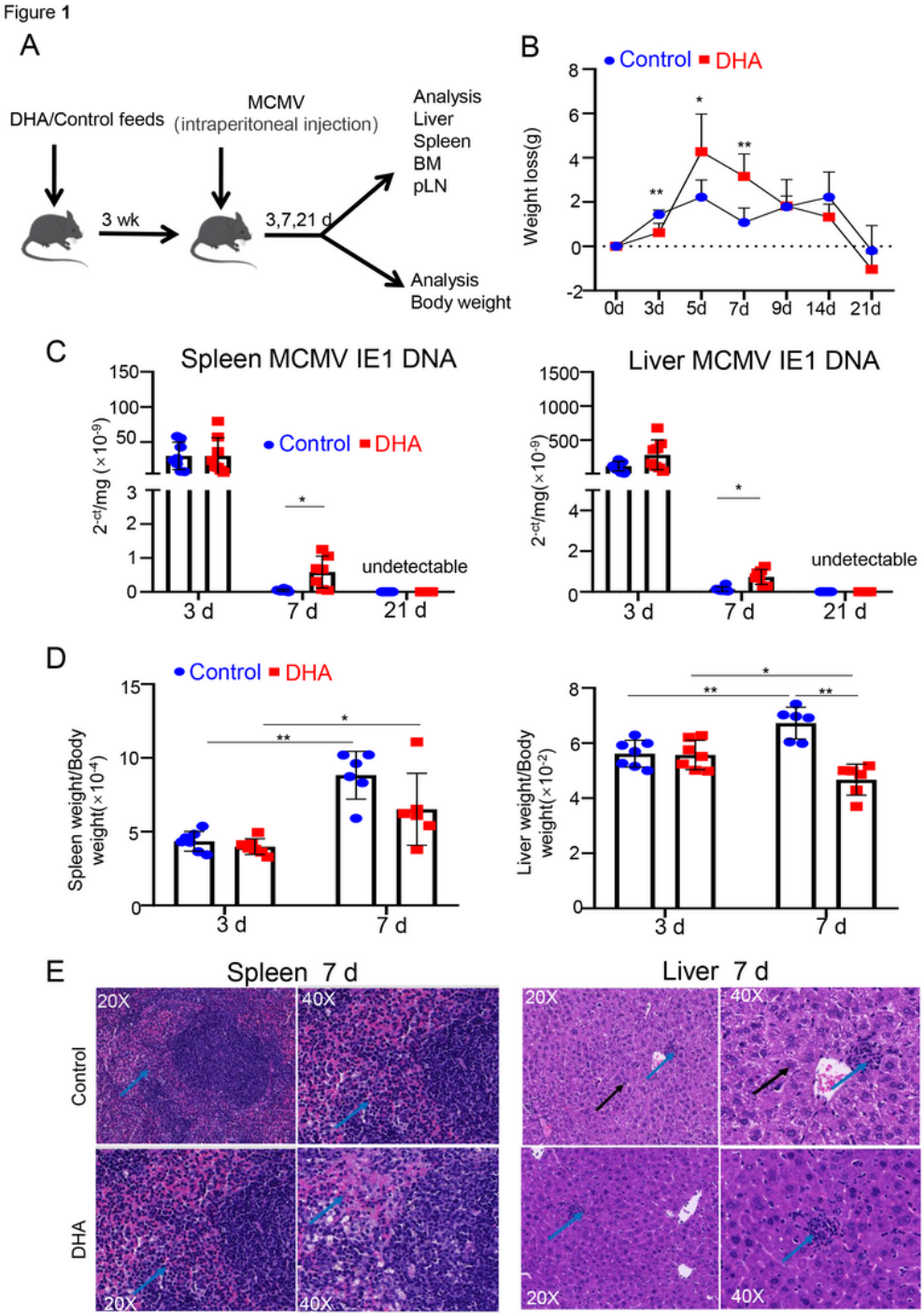

Figure 1

The effect of DHA feeding on MCMV resistance in C57BL/6J mice. A Schematic diagram of the experimental design. B Weight loss change in mice fed a DHA-supplemented or control diet on days 0, 3, 5, 7, 9, 14, and 21 after MCMV infection. C The MCMV IE-1 DNA level in the spleen (left) and liver (right) on days 3, 7, and 21 after MCMV infection was detected by qPCR. D The tissue/body weight ratio was calculated after weighing the spleen (left) and liver (right) tissues of mice fed a DHA-supplemented or

control diet on days 3 and 7 following MCMV infection. E H&E staining of the spleen and liver tissue at day 7 post MCMV infection. Black arrow indicated the cytoplasm is loose and weakly stained in hepatocytes, and blue arrows indicated lymphocytes accumulate in the focal area, respectively. Each symbol represents an individual mouse, and the blue dots and red square represent control and DHA-enriched diet-fed mice, respectively. All experiments were replicated at least 2 times. Error bars represent SDs; *, p<0.05; **, p <0.01.

Figure 2

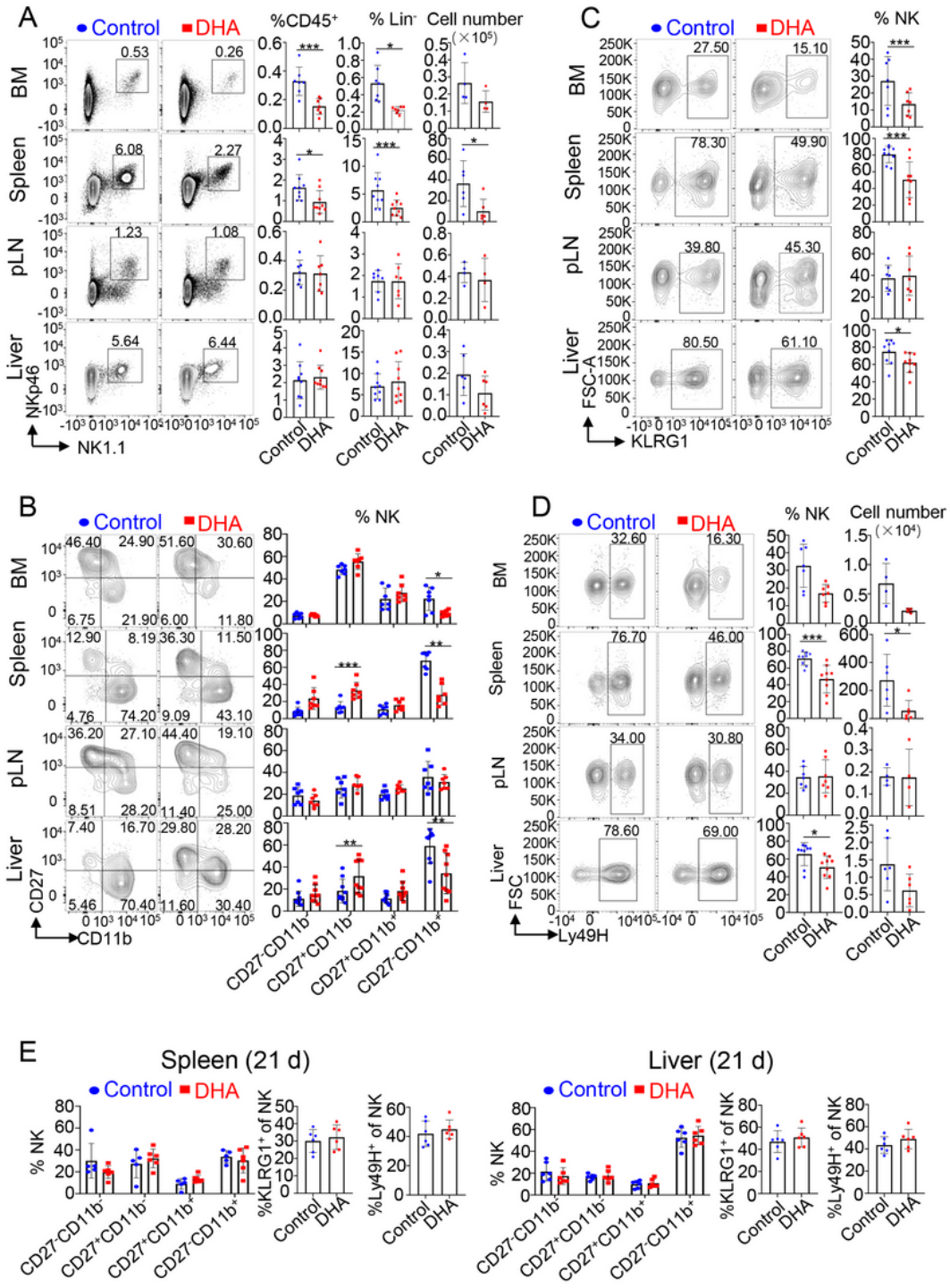

Figure 2

DHA feeding affected NK cell homeostasis, maturation and Ly49H+ NK cell expansion during the response to MCMV infection. A Flow cytometric analysis and enumeration of NK cells (CD45+CD3−CD19− NK1.1+NKp46+) in the BM, spleens, pLNs and livers of control versus DHA-fed mice. B Flow cytometric analysis and cumulative frequencies of subpopulations of NK cell (CD3−CD19−NK1.1+NKp46+) subsets based on CD11b and CD27 expression in the BM, spleens, pLNs and livers of control versus DHA-fed mice. C-D Flow cytometric analysis and enumeration of the KLRG1+ (C) and Ly49H+ (D) subsets of NK cells (CD3−CD19−NK1.1+NKp46+) in the BM, spleens, pLNs and livers of control versus DHA-fed mice on day 7 postinfection. E Cumulative frequencies of NK cell (CD3−CD19−NK1.1+NKp46+) subsets found in the BM, spleens, pLNs and livers of control versus DHA-fed mice on day 21 postinfection. Each symbol represents an individual mouse, and the blue dots and red square represent control and DHA-enriched diet-fed mice, respectively. All experiments were replicated at least 3 times. Error bars represent SDs; *, p<0.05; **, p <0.01; ***, p<0.001.

Figure 3

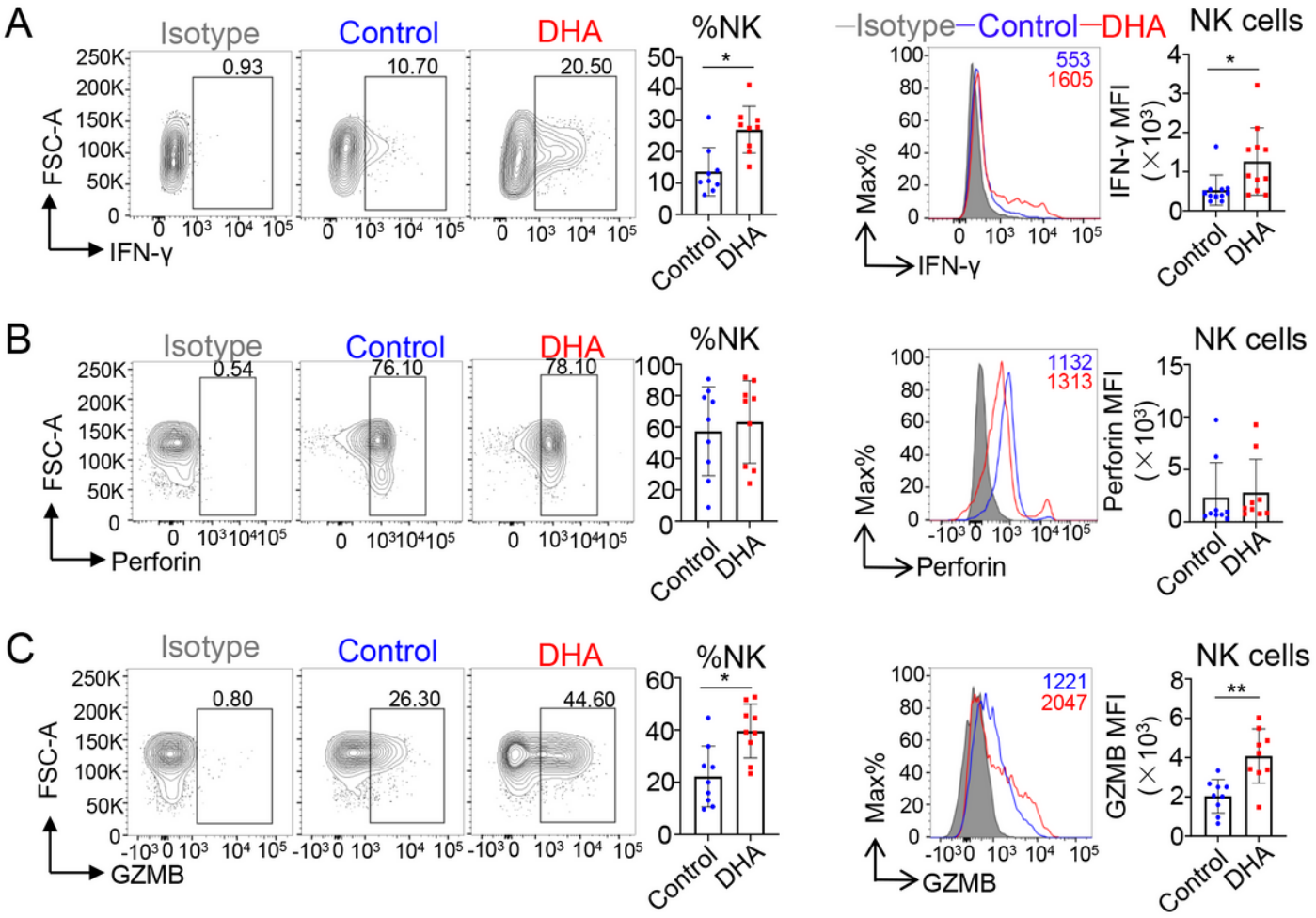

Figure 3

DHA feeding improved IFN-γ production and degranulation by NK cells in the spleen. A Flow cytometric analysis of the ratio and the mean fluorescence intensity (MFI) of IFN-γ+ splenic NK cells (CD3−CD19−NK1.1+NKp46+) from control versus DHA-fed mice following stimulation with PMA and

ionomycin in the presence of GolgiPlug for 6 h. B-C Flow cytometric analysis depicting the frequencies and MFI of perforin (B) and granzyme B (C) by splenic NK cells (CD3−CD19−NK1.1+NKp46+) from control versus DHA-fed mice on day 7 postinfection. Each symbol represents an individual mouse, and the blue dots and red square represent control and DHA-enriched diet-fed mice, respectively. All experiments were replicated at least 3 times. Error bars represent SDs; *, p<0.05; **, p <0.01.

Figure 4

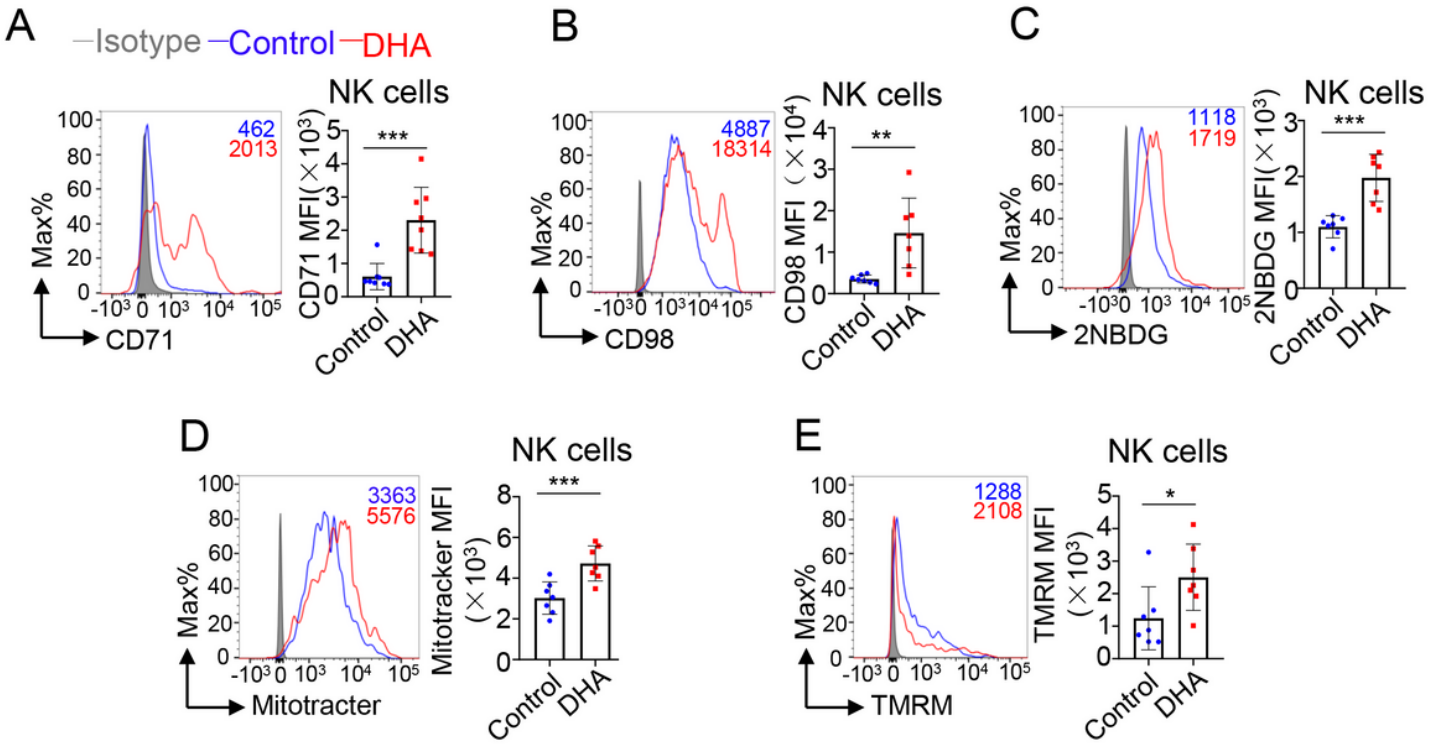

Figure 4

The difference in cellular metabolic status and mitochondrial activity of splenic NK cells between DHA-fed and control mice during MCMV infection. A-E Flow cytometric analysis and cumulative results depicting the MFI of CD98 (A) and CD71 (B) and the uptake of 2-NBDG (C), MitoTracker (D) and tetramethylrhodamine ethyl ester (TMRE) (E) by splenic NK cells (CD3−CD19−NK1.1+NKp46+) from control versus DHA-fed mice on day 7 postinfection. Each symbol represents an individual mouse, and the blue dots and red square represent control and DHA-enriched diet-fed mice, respectively. All experiments were replicated at least 3 times. Error bars represent SDs; *, p<0.05; **, p <0.01; ***, p<0.001.

Figure 5

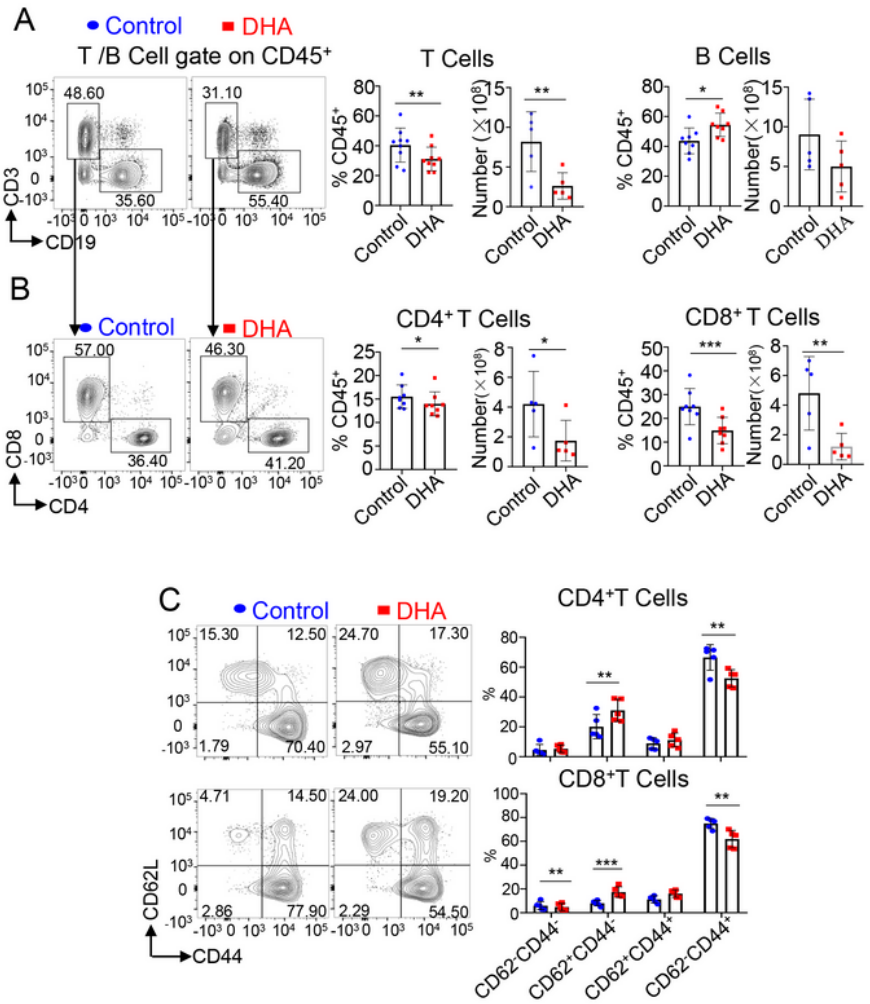

Figure 5

The effects of DHA feeding on the cellularity and activation of T and B cells in the spleen. A Flow cytometric analysis and enumeration of total T cells (CD45+CD3−CD19−), CD4+ T cells (CD45+CD3+CD19-CD4+CD8−), CD8+ T cells (CD45+CD3+CD19−CD4−CD8+) and B cells (CD45+CD3−CD19+) in the spleens of control versus DHA-fed mice. B Flow cytometric analysis and cumulative data indicating the expression of CD62L and CD44 in CD4+ T and CD8+ T cells between

control and DHA-fed mice. Each symbol represents an individual mouse, and the blue dots and red square represent control and DHA-enriched diet-fed mice, respectively. All experiments were replicated at least 3 times. Error bars represent SDs; *, p<0.05; **, p <0.01; ***, p<0.001.

Figure 6

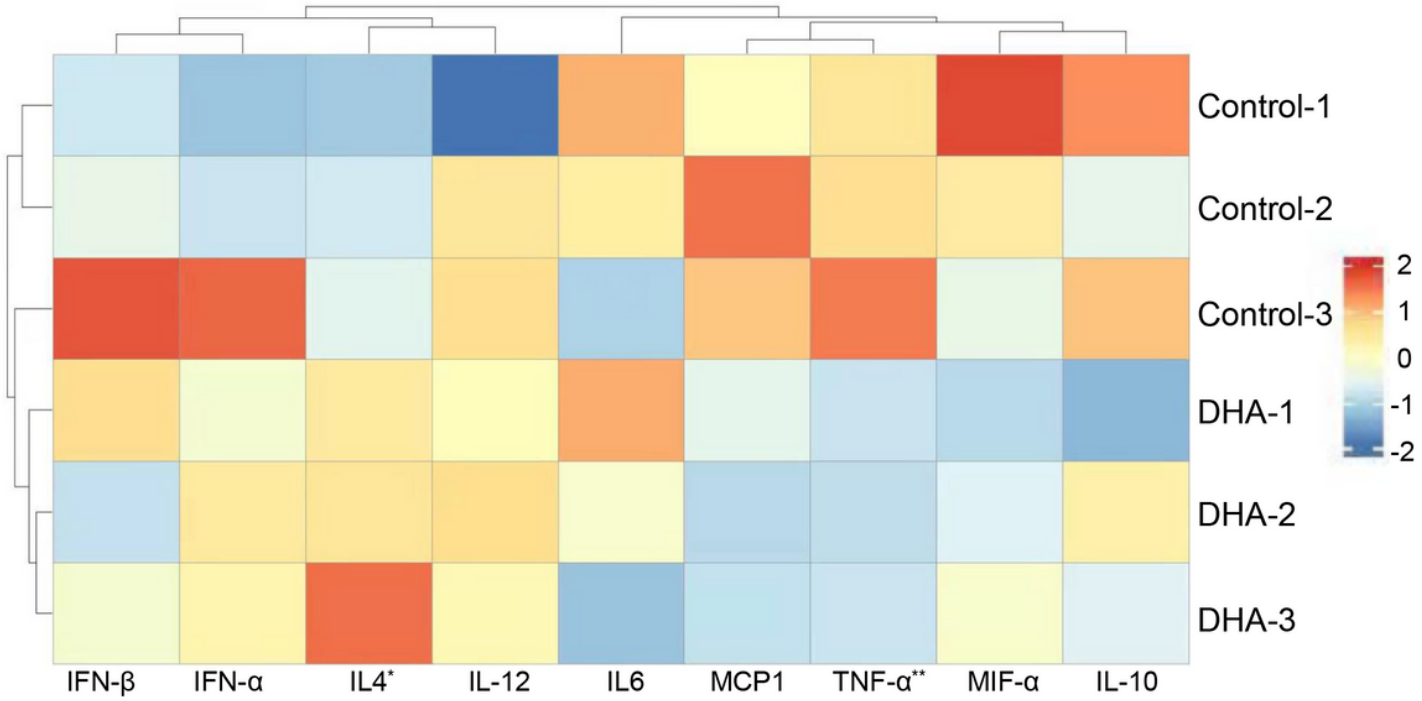

Figure 6

The effects of DHA feeding on the mRNA expression of inflammatory mediators after MCMV infection. On day 7 postinfection, the expression levels of the cytokines and chemokines IL4, IFN-β, MIP-1α, IL10, MCP.1, IL12, TNF-α, IFN- α, and IL6 in the spleens of control and DHA-fed mice were detected by qRT-PCR. Heatmap showing the relative expression of the indicated inflammatory mediators in the spleens from control and DHA-fed mice. *, p<0.05; **, p <0.01.